ACS Medicinal Chemistry Letters
Cite This: ACS Med. Chem. Lett. XXXX, XXX, XXX−XXX
Letter
pubs.acs.org/acsmedchemlett

Discovery of Pyrazolocarboxamides as Potent and Selective Receptor Interacting Protein 2 (RIP2) Kinase Inhibitors

Curt D. Haffner,[†] Adam K. Charnley,*[,†] Christopher J. Aquino,[§] Linda Casillas,[†] Máire A. Convery,[‡] Julie A. Cox,[†] Mark A. Elban,[†] Nicole C. Goodwin,[†] Peter J. Gough,[†] Pamela A. Haile,[†] Terry V. Hughes,[∥] Beth Knapp-Reed,[†] Constantine Kreatsoulas,[†] Ami S. Lakdawala,[†] Huijie Li,[†] Yiqian Lian,[†] David Lipshutz,[†] John F. Mehlmann,[†] Michael Ouellette,[†] Joseph Romano,[†] Lisa Shewchuk,[†] Arthur Shu,[†] Bartholomew J. Votta,[†] Huiqiang Zhou,[†] John Bertin,[†] and Robert W. Marquis[†]

[†]GlaxoSmithKline, 1250 South Collegeville Road, Collegeville, Pennsylvania 19426, United States
[‡]GlaxoSmithKline, Medicines Research Centre, Gunnels Wood Road, Stevenage, SG1 2NY, U.K.

Supporting Information

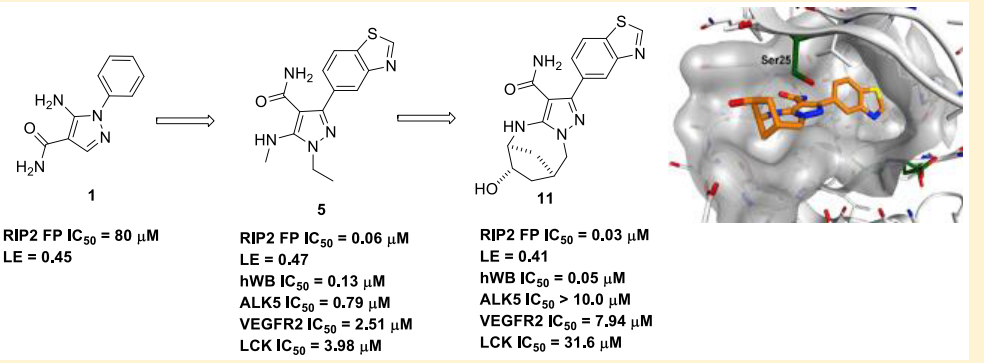

ABSTRACT: Herein we report the discovery of pyrazolocarboxamides as novel, potent, and kinase selective inhibitors of receptor interacting protein 2 kinase (RIP2). Fragment based screening and design principles led to the identification of the inhibitor series, and X-ray crystallography was used to inform key structural changes. Through key substitutions about the N1 and C5 N positions on the pyrazole ring significant kinase selectivity and potency were achieved. Bridged bicyclic pyrazolocarboxamide **11** represents a selective and potent inhibitor of RIP2 and will allow for a more detailed investigation of RIP2 inhibition as a therapeutic target for autoinflammatory disorders.

KEYWORDS: *Fragment based drug design (FBDD), receptor interacting protein 2 kinase, RIPK2, RIP2K, RIP2, nucleotide-binding oligomerization domain 1, NOD1, nucleotide-binding oligomerization domain 2, NOD2, ALK5, VEGFR2, LCK, structure based drug design (SBDD)*

The NOD-like receptors NOD1 and NOD2 (nucleotide-binding oligomerization domain-containing proteins 1 and 2) are cytosolic pattern recognition receptors (PRRs) that serve as bacterial sensors and mediate the host immune response. NOD1 and NOD2 bind distinct bacterial peptidoglycan components diaminopimelic acid (DAP) and muramyl dipeptide (MDP), respectively.[1−3] Upon binding their respective ligands, NOD1 or NOD2 recruit the serine/threonine kinase receptor interacting protein 2 kinase (RIP2 kinase), also known as RIPK2, CARD3, RICK, CARDIAK.[4−6] RIP2 kinase subsequently undergoes both autophosphorylation and polyubiquitination.[7−9] These modifications facilitate assembly of a signaling complex, activation of the canonical NF-kB and mitogen-activated protein kinase (MAPK) signaling pathways, and ultimately, production of multiple proinflammatory cytokines and chemokines.[10−12] Dysregulation of NOD/RIP2-dependent signaling has been linked to human disease, including asthma,[13] early onset inflammatory bowel disease,[14] sarcoidosis,[15] and Crohn's disease (CD).[16,17] Furthermore, activating mutations in the central nucleotide binding (NACHT) domain of NOD2 have been reported to cause Blau syndrome, an ultrarare autoinflammatory disease,[18] and increased expression of the activated/phosphorylated RIP2 kinase has been observed in intestinal biopsies taken from pediatric CD and ulcerative colitis (UC) patients with active disease.[19−22] Synergistic interactions of the NOD and TLR signaling pathways[23] expand the implications of modulating the NOD/RIP2 pathways.

Received: March 29, 2019
Accepted: September 26, 2019

DOI: 10.1021/acsmedchemlett.9b00141
ACS Med. Chem. Lett. XXXX, XXX, XXX−XXX

Recently, groups including ours have reported that small molecule RIP2 inhibitors block proinflammatory signaling and reduce inflammation in preclinical models.[24−29] Together, these data support the notion that the NOD/RIP2 signaling pathways likely play a significant role in the pathogenesis of inflammatory diseases and that specific targeting of this pathway may have broad therapeutic value.

In an effort to identify structurally diverse inhibitors of RIP2, we embarked on a fragment based screening and design program.[30] The FBDD effort began by screening a GSK fragment set designed around chemical motifs expected to interact in the ATP binding site of kinases. Screening roughly 1000 compounds through a fluorescence polarization binding assay[31] at 400 μM afforded 49 compounds with >50% inhibition. These were progressed into full curve analysis which gave IC_{50}'s ranging from 500−5 μM. All 49 fragments were progressed into a thermal melt stabilization assay to validate binding to RIP2. Gratifyingly, 30 of the hits confirmed binding in the thermal shift assay. From these, 27 fragments were progressed into crystallography experiments yielding 20 RIP2-fragment cocrystal structures. Careful analysis of the resultant cocrystal structures enabled clustering the fragments by key binding interactions and potential growth vectors. Hit-to-lead chemistry was initiated on five fragment series representing four different binding clusters. Ultimately, chemistry efforts were narrowed to a single fragment series derived from commercially available pyrazolocarboxamide **1a** (Figure 1).[32]

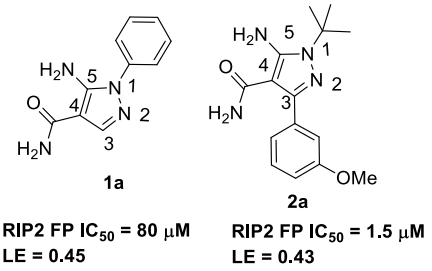

Figure 1. RIP2 inhibitor **1a** and data mining hit **2a**.

Fragment-to-lead efforts on the pyrazolocarboxamides began with a crystal structure of **1a**, which showed that the C4-amide makes two hinge binding H-bonds, the C5 amine (C5 N) interacts with the gatekeeper side-chain, and the N1-phenyl group projects to the kinase back pocket (Figure 2). Additional examination of the crystal structure revealed that the C3 position of the pyrazole offered a growth vector toward Ser25, a key glycine rich loop residue which makes interactions with other known RIP2 inhibitors and presents potential selectivity-driving interactions.[33] We envisioned growing off of this position of the fragment to incorporate an appropriately placed hydrogen bond acceptor in order to engage Ser25. Mining the GSK compound collection for related molecules with C3 substitution led to the identification of **2a**. This pyrazolocarboxamide compound contained aryl substitution at the C3 position with OMe as a potential Ser25-engaging group, and a bulky *tert*-butyl group at N1 as a putative replacement for phenyl back pocket binder. When we obtained a cocrystal structure of **2a**, we observed this compound had flipped in the pocket relative to our original fragment hit (Figure 2), with the C3 aryl occupying the back pocket and reversing the hinge and gatekeeper interactions.

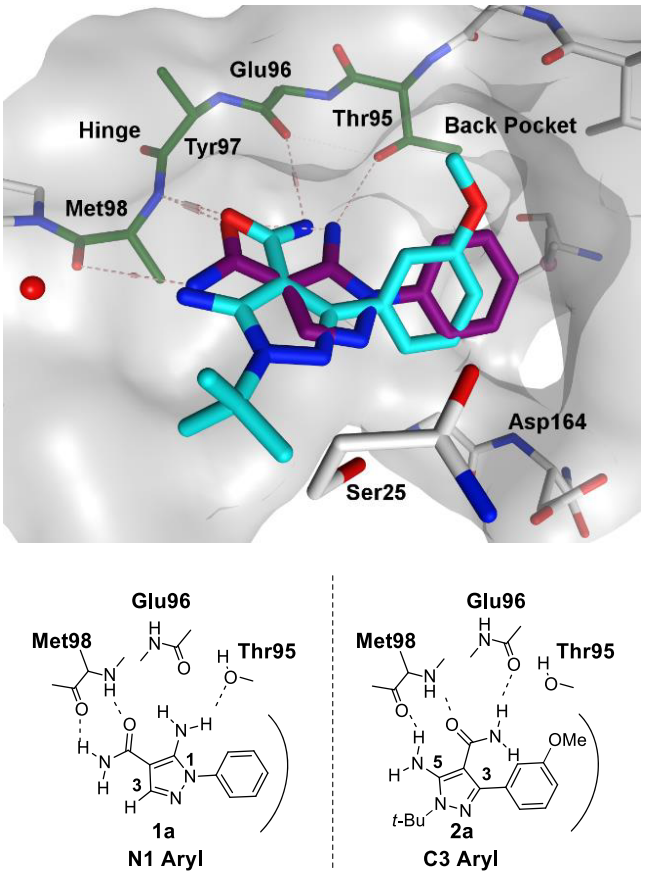

Figure 2. Overlay of pyrazolecarboxamides **1a** (plum) and **2a** (cyan) illustrating the two pyrazolocarboxamide binding modes.

To investigate the two pyrazolocarboxamide binding modes, we synthesized several sets of matched pairs that swapped the C3 and N1 substitutions. As shown in Table 1, the C3 aryl

Table 1. In Vitro Potency Data for Compounds 2a−f and 3a−f[a]

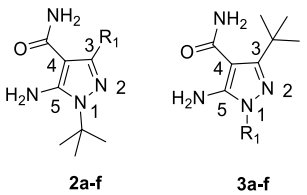

	RIP2 FP IC_{50}	
R_1	C3 aryl	N1 aryl
3-methoxyphenyl	**2a**	**3a**
	1.6[b]	32[c]
4-chloro-3-methoxyphenyl	**2b**	**3b**
	0.08[b]	20[c]
m-tolyl	**2c**	**3c**
	5.0[c]	25[c]
3,4-dichlorophenyl	**2d**	**3d**
	0.12[b]	>10[c]
1H-indazol-5-yl	**2e**	**3e**
	1.2[c]	25[c]
2-naphthalenyl	**2f**	**3f**
	0.06[b]	50[c]

[a]IC_{50} values in μM. [b]$n \geq 6$. [c]$n = 2$.

DOI: 10.1021/acsmedchemlett.9b00141
ACS Med. Chem. Lett. XXXX, XXX, XXX−XXX

compounds (see **2a−f**) were significantly more potent compared to their N1 aryl counterparts (**3a−f**), even though the molecules can engage the same residues along the hinge and place an aryl group in the back pocket, regardless of orientation of the pyrazole ring. We hypothesize that these potency differences can be attributed to electronic differences in the interactions between the pyrazole C5 amine and C4 amide with Met98, Glu96, and Thr95. Subtle differences in the placement of the back pocket aryl group between the two motifs also likely contribute to the potency differences. Among the C3 aryl substituents, we were able to increase potency by filling the back pocket with substitution at the 3-position (**2c**), 3,4-disubstitution (**2d**), and fused bicycles (**2e−f**). Of these inhibitors, **2f** was the most potent but suffered from poor solubility. The crystal structures of the C3 aryls suggested that an appropriately placed hydrogen bond acceptor could engage with the backbone NH of Asp164. With this in mind, we designed a set of heterocyclic back pocket groups that would test this hypothesis and hopefully improve solubility. Gratifyingly, benzothiazole **2k** offered a nice balance of potency and improved physicochemical properties (Table 2).

Table 2. In Vitro Potency Data for Compounds 2g−k[a]

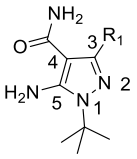

2g-k

	RIP2 FP IC_{50}
R_1	C3 aryl
benzo[d][1,3]dioxol-5-yl	**2g** 0.79[b]
benzo[c][1,2,5]oxadiazol-5-yl	**2h** 0.79[d]
1H-benzo[d]imidazol-5-yl	**2i** 3.2[c]
1H-indol-6-yl	**2j** 0.12[c]
benzo[d]thiazol-5-yl	**2k** 0.04[b]

[a]IC_{50} values in μM. [b]$n \geq 6$. [c]$n = 2$. [d]$n = 4$.

With the discovery of **2k**, the program transitioned from a hit-to-lead effort to a lead optimization program. A primary point of optimization was inhibition activity in human whole blood (hWB) and kinase selectivity. The team chose to fix the back pocket group as benzothiazole and explore the impact of N1/C5 N substitution (Table 3). Converting the *tert*-butyl to an ethyl group, maintained RIP2 binding activity (compound **4**) but had reduced human whole blood (hWB) activity.[34] The addition of a methyl group onto the exocyclic nitrogen attached to C5 afforded **5** and a substantial improvement in whole blood activity. Additionally, selectivity against three key sentinel kinases (activin receptor-like kinase 5 - ALK5, vascular endothelial growth factor receptor 2 - VEGFR2, and lymphocyte-specific protein tyrosine kinase - LCK) was improved relative to **2k** and **4**.

This profile identified **5**, and more broadly C5 N alkyls, as an attractive inhibitor series. Screening of activity against a broad panel of kinases suggested reasonable off-target kinase

Table 3. Lead Optimization SAR on N1/C5 N Substitution[a,24]

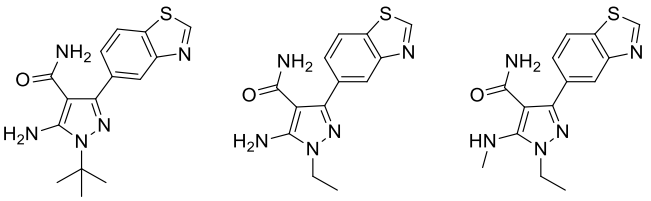

2k **4** **5**

	GSK′583	2k	4	5
RIP2 FP IC_{50}	0.005[24]	0.04[b]	0.05[c]	0.06[b]
hWB IC_{50}	0.237[24]	0.54[b]	0.64[c]	0.12[b]
ALK5 IC_{50}	3.16[e]	0.32[b]	0.32[c]	0.79[b]
VEGFR2 IC_{50}	>5.0[24]	0.25[f]	0.40[c]	2.51[b]
LCK IC_{50}	12.6[b]	0.25[b]	1.00[d]	3.98[b]

[a]Known RIP2 inhibitor GSK′583 is included for reference. IC_{50} values in μM. [b]$n \geq 6$. [c]$n = 2$. [d]$n = 3$. [e]$n = 4$. [f]$n = 5$.

selectivity.[35,36] Importantly, **5** also possessed a suitable oral pharmacokinetic profile in rat (data not shown). The activity in hWB combined with oral exposure made **5** the first progressible molecule from the pyrazolocarboxamide class, and it was profiled in a seven day rat safety assessment study. Unfortunately, substantial toxicity findings precluded further progression of this compound.

With the goal to identify a clinical candidate from the pyrazolecarboxamide series, the team set out to identify an inhibitor that demonstrated both improved selectivity and potency, setting a goal of at least 100-fold biochemical selectivity against the sentinel kinases (ALK5, VEGFR2, LCK) and whole blood activity <100 nM.

Leveraging our in-house crystallography to generate numerous RIP2 cocrystal structures with our pyrazolocarboxamide inhibitors,[24,25,33] we set out to rationally improve the RIP2 affinity and selectivity of our molecules. One approach we employed was to install a covalent linkage between the N1 and C5 substitutions. This would also enable further substitution as dictated by the biochemical data. Therefore, three N1−C5 cyclized analogs were synthesized to probe the SAR spanning six to eight membered rings (Table 4). The six-

Table 4. In Vitro Potency and Selectivity Data for Compounds 5−9[a]

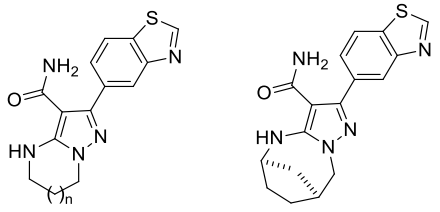

6 - 8 **9**

compound	5	6	7	8	9
n		1	2	3	
RIP2 FP IC_{50}	0.06[b]	0.25[f]	0.06[b]	0.025[d]	0.05[d]
RIP2 hWB IC_{50}	0.12[b]	1.15[b]	0.70[d]	0.37[d]	0.29[d]
ALK5 IC_{50}	0.79[b]	3.16[d]	3.98[f]	1.26[f]	>10.0[f]
VEGFR2 IC_{50}	2.51[b]	7.94[d]	2.51[f]	3.2[f]	5.01[e]
LCK IC_{50}	3.98[b]	10.0[c]	3.16[d]	10.0[d]	7.94[d]

[a]IC_{50} values in μM. [b]$n \geq 6$. [c]$n = 1$. [d]$n = 2$. [e]$n = 3$. [f]$n = 4$.

DOI: 10.1021/acsmedchemlett.9b00141
ACS Med. Chem. Lett. XXXX, XXX, XXX−XXX

membered ring compound **6** was found to be less potent than compound **5** (FP IC_{50} = 250 nM), and the selectivity window to ALK5, VEGFR2, and LCK remained the same. Interestingly, the 7-membered ring compound **7** retained the same RIP2 biochemical potency as compound **5** (IC_{50} = 60 nM) but became 5-fold more selective against ALK5 (no significant change was observed against VEGFR2 and LCK). Finally, the 8-membered ring analog, compound **8**, demonstrated the best biochemical activity with an IC_{50} = 25 nM versus RIP2. Importantly, the kinase selectivity window also widened with the best improvement seen against LCK. A cocrystal structure was solved with compound **6** (data not shown) which was used to design additional interactions with the protein via proper placement of substituents off of the tether. In particular, by projecting out of the plane of the bicyclic ring, hydrophobic interactions with Leu24 and Leu153 may be realized. Accordingly, a bridged bicyclic analog, **9**, was designed and synthesized. This compound was found to have similar biochemical potency to compound **7** (Table 4). The most striking piece of data was the loss of ALK5 activity. The selectivity window against all three kinases was now ≥100-fold. However, the desired whole blood potency was still lacking.

Given the kinase selectivity success achieved with the bridged bicyclic analog **9**, we expanded on this SAR using guidance from our cocrystal structure of **6**. In particular, we targeted a hydrogen bonding interaction with Ser25 via strategically placed hydroxyl groups on the ethano bridge. Supporting this strategy, only three known kinases have a serine in this position,[37] and the bridging saturated ring sits beneath the loop containing Ser25. We hypothesized that installation of this functionality would improve potency through an additional interaction with the protein and further widen the kinase selectivity. To investigate this SAR, four analogs were synthesized containing a hydroxyl moiety on the ethano bridge (Table 5). Compound **10** was found to have similar potency to **9**, and no activity was observed at the highest concentration against all three sentinel kinases. The hWB IC_{50} for this compound was comparable to compound **9**. Compound **11**, the enantiomer of **10**, was the most potent within the series (IC_{50} = 30 nM) and, like **10**, showed very good kinase selectivity. Interestingly, the hWB potency was also improved (IC_{50} = 50 nM). Compound **13** was less active than either **10** or **11** but was again quite selective, and the least active compound was **12** (enantiomer of **13**). All hydroxyl compounds demonstrated good selectivity. A crystal structure of compound **11** was obtained (Figure 3), yet examination of this structure revealed that the hydroxyl residue is directed toward solvent and makes no key interactions with the protein. Interestingly, the hydroxyl moiety on **13** was within 2.6 Å of Ser25, as designed (a cocrystal structure was solved), suggesting that this interaction was not critical in driving RIP2 affinity, yet impacting the whole blood activity of the molecule.

Table 5. In Vitro Potency and Selectivity Data for Compounds 10−13[a]

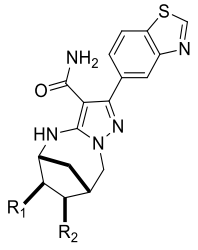

10 R_1 = OH, R_2 = H
12 R_1 = H, R_2 = OH

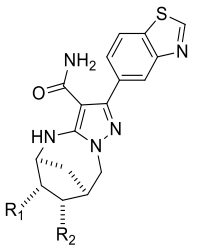

11 R_1 = OH, R_2 = H
13 R_1 = H, R_2 = OH

	10	11	12	13
RIP2 FP IC_{50}	0.06[d]	0.03[b]	0.16[d]	0.08[e]
hWB IC_{50}	0.28[d]	0.05[b]	0.22[d]	0.19[d]
ALK5 IC_{50}	>10.0[f]	>10.0[b]	>10.0[d]	>10.0[b]
VEGFR2 IC_{50}	>10.0[f]	7.94[f]	>10.0[f]	>10.0[b]
LCK IC_{50}	>31.0[c]	31.6[d]	>31.0[d]	>31.0[d]

[a]IC_{50} values in μM. [b]$n \geq 6$. [c]$n = 1$. [d]$n = 2$. [e]$n = 3$. [f]$n = 4$.

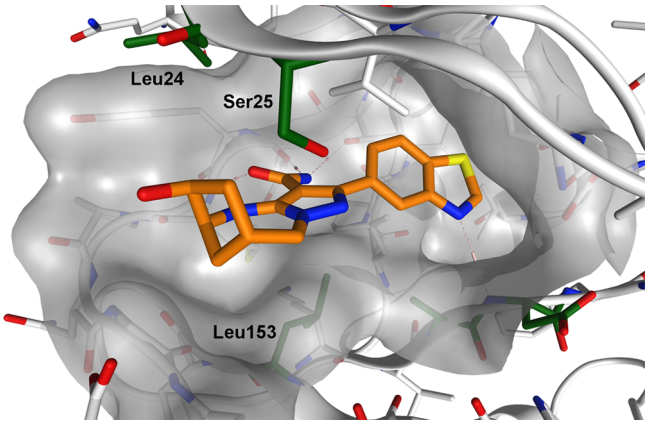

Figure 3. Cocrystal structure of RIP2 with bridged bicyclic inhibitor **11**.

Given both **11** and **12** direct their hydroxyl groups toward solvent (**12** based on modeling), the roughly 5-fold biochemical potency difference between **11** and **12** could be due to the increased hydrophobic interactions of the ethano versus methano bridge with the hydrophobic loop of the protein. The hWB potency for compound **11**, as mentioned above, was substantially better than the other three compounds, yet it is unclear what is driving this difference. Importantly, compound **11** achieved both the potency and selectivity criteria established for a follow up to **5**.

In conclusion, fragment-based screening and drug design delivered an efficient lead series of RIP2 inhibitors (LE = 0.43 for **2a**, 0.47 for **5**, and 0.41 for **11**).[32] By employing fragment evolution principles, robust crystallography, and structure-based design, we converted hit **1** to bridged bicyclic pyrazolcarboxamide **11**. This compound combines excellent biochemical and whole blood activity with kinase selectivity[38] and promises to enable investigation of RIP2 inhibition as a viable modality for the treatment of inflammatory indications.

■ ASSOCIATED CONTENT

Supporting Information

The Supporting Information is available free of charge on the ACS Publications website at DOI: 10.1021/acsmedchemlett.9b00141.

Experimentals procedures for the preparation of all compounds PDF)

DOI: 10.1021/acsmedchemlett.9b00141
ACS Med. Chem. Lett. XXXX, XXX, XXX−XXX

AUTHOR INFORMATION

Corresponding Author

*E-mail: adam.k.charnley@gsk.com.

ORCID

Adam K. Charnley: 0000-0003-1188-1715
Nicole C. Goodwin: 0000-0002-6093-7175
Pamela A. Haile: 0000-0003-3950-4890

Present Addresses

[§](C.J.A.) CJAMedChem, LLC, 1600 W. Bromfield Dr., Hillsborough, NC 27599, United States.
[‖](T.V.H.) Janssen Research & Development LLC, P.O. Box 776, Spring House, PA 19477, United States.

Author Contributions

The manuscript was written through contributions of all authors. All authors have given approval to the final version of the manuscript.

Notes

The authors declare no competing financial interest.

ACKNOWLEDGMENTS

We would like to thank Karl Erhard for the assistance in optimizing the purification of compound **11** and the Protein & Cellular Sciences, MST, for protein production.

ABBREVIATIONS

RIP2, receptor interacting protein 2 kinase; NOD1, nucleotide-binding oligomerization domain 1; NOD2, nucleotide-binding oligomerization domain 2; ALK5, activin-like kinase 5; VEGFR2, vascular endothelial growth factor receptor 2; LCK, lymphocyte-specific protein tyrosine kinase

REFERENCES

(1) Philpott, D. J.; Sorbara, M. T.; Robertson, S. J.; Croitoru, K.; Girardin, S. E. NOD proteins: regulators of inflammation in health and disease. *Nat. Rev. Immunol.* **2014**, *14* (1), 9−23.

(2) Girardin, S. E.; Boneca, I. G.; Viala, J.; Chamaillard, M.; Labigne, A.; Thomas, G.; Philpott, D. J.; Sansonetti, P. J. NOD2 is a general sensor of peptidoglycan through muramyldipeptide (MDP) detection. *J. Biol. Chem.* **2003**, *278*, 8869−8872.

(3) Girardin, S. E.; Boneca, I. G. J.; Carneiro, A. M.; Antignac, A.; Jehanno, M.; Viala, J.; Tedin, K.; Taha, M.-K.; Labigne, A.; Zathringer, U.; Coyle, A. J.; DiStefano, P. S.; Bertin, J.; Sansonetti, P. J.; Philpott, D. J. NOD1 detects a unique muropeptide from gram-negative bacterial peptidoglycan. *Science* **2003**, *300*, 1584−1587.

(4) McCarthy, J. V.; Ni, J.; Dixit, V. M. RIP2 is a novel NF-κB-activating and cell death-inducing kinase. *J. Biol. Chem.* **1998**, *273*, 16968−16975.

(5) Inohara, N.; Del Peso, L.; Koseki, T.; Chen, S.; Nunez, G. J. RICK, a novel protein kinase containing a caspase recruitment domain, interacts with CLARP and regulates CD95-mediated apoptosis. *J. Biol. Chem.* **1998**, *273*, 12296−12300.

(6) Irving, A. T.; Mimuro, H.; Kufer, T. A.; Lo, C.; Wheeler, R.; Turner, L. J.; Thomas, B. J.; Malosse, C.; Gantier, M. P.; Casillas, L. N.; Votta, B. J.; Bertin, J.; Boneca, I. G.; Sasakawa, C.; Philpott, D. J.; Ferrero, R.; Kaparakis-Liakos, M. The immune receptor NOD1 and kinase RIP2 interact with bacterial peptidoglycan on early endosomes to promote autophagy and inflammatory signaling. *Cell Host Microbe* **2014**, *15*, 623−635.

(7) Mayle, S.; Boyle, J. P.; Sekine, E.; Zurek, B.; Kufer, T. A.; Monie, T. P. Engagement of nucleotide-binding oligomerization domain-containing protein 1 (NOD1) by receptor-interacting protein 2 (RIP2) is insufficient for signal transduction. *J. Biol. Chem.* **2014**, *289* (33), 22900−22914.

(8) Dorsch, M.; Wang, A.; Cheng, H.; Lu, C.; Bielecki, A.; Charron, K.; Clauser, K.; Ren, H.; Polakiewicz, R. D.; Parsons, T.; Li, P.; Ocain, T.; Xu, Y. Identification of a regulatory autophosphorylation site in the serine-threonine kinase RIP2. *Cell. Signalling* **2006**, *18* (12), 2223−2229.

(9) Hasegawa, M.; Fujimoto, Y.; Lucas, P. C.; Nakano, H.; Fukase, K.; Nunez, G.; Inohara, N. A critical role of RICK/RIP2 polyubiquitination in Nod-induced NF-kappaB activation. *EMBO J.* **2008**, *27* (2), 373−383.

(10) Windheim, M.; Lang, C.; Peggie, M.; Plater, L. A.; Cohen, P. Molecular mechanisms involved in the regulation of cytokine production by muramyl dipeptide. *Biochem. J.* **2007**, *404* (2), 179−190.

(11) Tigno-Aranjuez, J. T.; Asara, J. M.; Abbott, D. W. Inhibition of RIP2's tyrosine kinase activity limits NOD2-driven cytokine responses. *Genes Dev.* **2010**, *24* (23), 2666−2677.

(12) Pellegrini, E.; Desfosses, A.; Wallmann, A.; Schulze, W. M.; Rehbein, K.; Mas, P.; Signor, L.; Gaudon, S.; Zenkeviciute, G.; Hons, M.; Malet, H.; Gutsche, I.; Sachse, C.; Schoehn, G.; Oschkinat, H.; Cusack, S. RIP2 filament formation is required for NOD2 dependent NF-kappaB signalling. *Nat. Commun.* **2018**, *9* (1), 4043.

(13) Hysi, P.; Kabesch, M.; Moffatt, M. F.; Schedel, M.; Carr, D.; Zhang, Y.; Boardman, B.; von Mutius, E.; Weiland, S. K.; Leupold, W.; Fritzsch, C.; Klopp, N.; Musk, A. W.; James, A.; Nunez, G.; Inohara, N.; Cookson, W. O. NOD1 variation, immunoglobulin E and asthma. *Hum. Mol. Genet.* **2005**, *14* (7), 935−41.

(14) McGovern, D. P.; Hysi, P.; Ahmad, T.; van Heel, D. A.; Moffatt, M. F.; Carey, A.; Cookson, W. O.; Jewell, D. P. Association between a complex insertion/deletion polymorphism in NOD1 (CARD4) and susceptibility to inflammatory bowel disease. *Hum. Mol. Genet.* **2005**, *14* (10), 1245−1250.

(15) Tanabe, T.; Ishige, I.; Suzuki, Y.; Aita, Y.; Furukawa, A.; Ishige, Y.; Uchida, K.; Suzuki, T.; Takemura, T.; Ikushima, S.; Oritsu, M.; Yokoyama, T.; Fujimoto, Y.; Fukase, K.; Inohara, N.; Nunez, G.; Eishi, Y. Sarcoidosis and NOD1 variation with impaired recognition of intracellular Propionibacterium acnes. *Biochim. Biophys. Acta, Mol. Basis Dis.* **2006**, *1762* (9), 794−801.

(16) Lesage, S.; Zouali, H.; Cezard, J. P.; Colombel, J. F.; Belaiche, J.; Almer, S.; Tysk, C.; O'Morain, C.; Gassull, M.; Binder, V.; Finkel, Y.; Modigliani, R.; Gower-Rousseau, C.; Macry, J.; Merlin, F.; Chamaillard, M.; Jannot, A. S.; Thomas, G.; Hugot, J. P.; Group, E.-I.; Group, E.; Group, G. CARD15/NOD2 mutational analysis and genotype-phenotype correlation in 612 patients with inflammatory bowel disease. *Am. J. Hum. Genet.* **2002**, *70* (4), 845−857.

(17) Hugot, J. P.; Chamaillard, M.; Zouali, H.; Lesage, S.; Cezard, J. P.; Belaiche, J.; Almer, S.; Tysk, C.; O'Morain, C. A.; Gassull, M.; Binder, V.; Finkel, Y.; Cortot, A.; Modigliani, R.; Laurent-Puig, P.; Gower-Rousseau, C.; Macry, J.; Colombel, J. F.; Sahbatou, M.; Thomas, G. Association of NOD2 leucine-rich repeat variants with susceptibility to Crohn's disease. *Nature* **2001**, *411* (6837), 599−603.

(18) Rose, C. D.; Martin, T. M.; Wouters, C. H. Blau syndrome revisited. *Curr. Opin. Rheumatol.* **2011**, *23*, 411−418.

(19) Strober, W.; Asano, N.; Fuss, I.; Kitani, A.; Watanabe, T. Cellular and molecular mechanisms underlying NOD2 risk-associated polymorphisms in Crohn's disease. *Immunol Rev.* **2014**, *260* (1), 249−260.

(20) Stronati, L.; Negroni, A.; Pierdomenico, M.; D'Ottavio, C.; Tirindelli, D.; Di Nardo, G.; Olivia, S.; Viola, F.; Cucchiara, S. Altered expression of innate immunity genes in different intestinal sites of children with ulcerative colitis. *Dig. Liver Dis.* **2010**, *42*, 848−853.

(21) Stronati, L.; Negroni, A.; Merola, P.; Pannone, V.; Borrelli, O.; Cirulli, M.; Annese, V.; Cucchiara, S. Mucosal NOD2 expression and NF-kappaB activation in pediatric Crohn's disease. *Inflamm Bowel Dis* **2008**, *14* (3), 295−302.

(22) Negroni, A.; Stronati, L.; Pierdomenico, M.; Tirindelli, D.; Di Nardo, G.; Mancini, V.; Maiella, G.; Cucchiara, S. Activation of NOD2-mediated intestinal pathway in a pediatric population with Crohn's disease. *Inflamm. Bowel Dis* **2009**, *15*, 1145−1154.

DOI: 10.1021/acsmedchemlett.9b00141
ACS Med. Chem. Lett. XXXX, XXX, XXX−XXX

(23) Pashenkov, M. V.; Murugina, N. E.; Budikhina, A. S.; Pinegin, B. V. Synergistic interactions between NOD receptors and TLRs: Mechanisms and clinical implications. *J. Leukocyte Biol.* **2019**, *105*, 1−12.
(24) Haile, P. A.; Votta, B. J.; Marquis, R. W.; Bury, M. J.; Mehlmann, J. F.; Singhaus, R., Jr.; Charnley, A. K.; Lakdawala, A. S.; Convery, M. A.; Lipshutz, D. B.; Desai, B. M.; Swift, B.; Capriotti, C. A.; Berger, S. B.; Mahajan, M. K.; Reilly, M. A.; Rivera, E. J.; Sun, H. H.; Nagilla, R.; Beal, A. M.; Finger, J. N.; Cook, M. N.; King, B. W.; Ouellette, M. T.; Totoritis, R. D.; Pierdomenico, M.; Negroni, A.; Stronati, L.; Cucchiara, S.; Ziolkowski, B.; Vossenkamper, A.; MacDonald, T. T.; Gough, P. J.; Bertin, J.; Casillas, L. N. The Identification and Pharmacological Characterization of 6-(tert-Butylsulfonyl)-N-(5-fluoro-1H-indazol-3-yl)quinolin-4-amine (GSK583), a Highly Potent and Selective Inhibitor of RIP2 Kinase. *J. Med. Chem.* **2016**, *59* (10), 4867−4880.
(25) Haile, P. A.; Casillas, L. N.; Bury, M. J.; Mehlmann, J. F.; Singhaus, R., Jr.; Charnley, A. K.; Hughes, T. V.; DeMartino, M. P.; Wang, G. Z.; Romano, J. J.; Dong, X.; Plotnikov, N. V.; Lakdawala, A. S.; Convery, M. A.; Votta, B. J.; Lipshutz, D. B.; Desai, B. M.; Swift, B.; Capriotti, C. A.; Berger, S. B.; Mahajan, M. K.; Reilly, M. A.; Rivera, E. J.; Sun, H. H.; Nagilla, R.; LePage, C.; Ouellette, M. T.; Totoritis, R. D.; Donovan, B. T.; Brown, B. S.; Chaudhary, K. W.; Gough, P. J.; Bertin, J.; Marquis, R. W. Identification of Quinoline-Based RIP2 Kinase Inhibitors with an Improved Therapeutic Index to the hERG Ion Channel. *ACS Med. Chem. Lett.* **2018**, *9* (10), 1039−1044.
(26) Tigno-Aranjuez, J. T.; Benderitter, P.; Rombouts, F.; Deroose, F.; Bai, X.; Mattioli, B.; Cominelli, F.; Pizarro, T. T.; Hoflack, J.; Abbott, D. W. In vivo inhibition of RIPK2 kinase alleviates inflammatory disease. *J. Biol. Chem.* **2014**, *289* (43), 29651−29664.
(27) Canning, P.; Ruan, Q.; Schwerd, T.; Hrdinka, M.; Maki, J. L.; Saleh, D.; Suebsuwong, C.; Ray, S.; Brennan, P. E.; Cuny, G. D.; Uhlig, H. H.; Gyrd-Hansen, M.; Degterev, A.; Bullock, A. N. Inflammatory Signaling by NOD-RIPK2 Is Inhibited by Clinically Relevant Type II Kinase Inhibitors. *Chem. Biol.* **2015**, *22* (9), 1174−1184.
(28) He, X.; Da Ros, S.; Nelson, J.; Zhu, X.; Jiang, T.; Okram, B.; Jiang, S.; Michellys, P. Y.; Iskandar, M.; Espinola, S.; Jia, Y.; Bursulaya, B.; Kreusch, A.; Gao, M. Y.; Spraggon, G.; Baaten, J.; Clemmer, L.; Meeusen, S.; Huang, D.; Hill, R.; Nguyen-Tran, V.; Fathman, J.; Liu, B.; Tuntland, T.; Gordon, P.; Hollenbeck, T.; Ng, K.; Shi, J.; Bordone, L.; Liu, H. Identification of Potent and Selective RIPK2 Inhibitors for the Treatment of Inflammatory Diseases. *ACS Med. Chem. Lett.* **2017**, *8* (10), 1048−1053.
(29) Goncharov, T.; Hedayati, S.; Mulvihill, M. M.; Izrael-Tomasevic, A.; Zobel, K.; Jeet, S.; Fedorova, A. V.; Eidenschenk, C.; deVoss, J.; Yu, K.; Shaw, A. S.; Kirkpatrick, D. S.; Fairbrother, W. J.; Deshayes, K.; Vucic, D. Disruption of XIAP-RIP2 Association Blocks NOD2-Mediated Inflammatory Signaling. *Mol. Cell* **2018**, *69* (4), 551−565.
(30) For a discussion of fragment based drug design see: Davis, B. J.; Roughley, S. D. Chapter Eleven − Fragment-Based Lead Discovery. *Annu. Rep. Med. Chem.* **2017**, *50*, 371−439. (a) Erlanson, D. A.; Fesik, S. W.; Hubbard, R. E.; Jahnke, W.; Jhoti, H. Twenty years on: the impact of fragments on drug discovery. *Nat. Rev. Drug Discovery* **2016**, *15*, 605−619.
(31) Parker, G. J.; Law, T. L.; Lenoch, F. J.; Bolger, R. E. Development of high throughput screening assays using fluorescence polarization: nuclear receptor-ligand-binding and kinase/phosphatase assays. *J. Biomol. Screening* **2000**, *5*, 77−88.
(32) Ligand Efficiancy (LE) = $1.4(-\log IC_{50})/N$ where N is the number of heavy atoms.
(33) Charnley, A. K.; Convery, M. A.; Kakdawala Shah, A.; Jones, E.; Hardwicke, P.; Bridges, A.; Ouellette, M.; Totoritis, R.; Schwartz, B.; King, B. W.; Wisnoski, D. D.; Kang, J.; Eidam, P. M.; Votta, B. J.; Gough, P. J.; Marquis, R. W.; Bertin, J.; Casillas, L. Crystal structures of human RIP2 kinase catalytic domain complexed with ATP-competitive inhibitors: Foundations for understanding inhibitor selectivity. *Bioorg. Med. Chem.* **2015**, *23*, 7000−7006.
(34) The human whole blood assay was used to measure cytokine production and is detailed in the Supporting Information.
(35) Selectivity against 300 human kinases for compound **5** was conducted at Reaction Biology Corporation and found to inhibit 6 kinases ≥ 70% @ 1 μM. See the Supporting Information.
(36) VEGFR2 data for GSK′583 was derived from a different *in vitro* biochemical assay than that reported for the compounds in this paper.
(37) Buzko, O.; Shokat, K. M. A kinase sequence database: sequence alignments and family assignment. *Bioinformatics* **2002**, *18*, 1274−1275.
(38) Selectivity against 366 human kinases for compound **11** was conducted at Reaction Biology Corporation and found to inhibit 1 kinase ≥ 70% @ 1 μM. See the Supporting Information.

DOI: 10.1021/acsmedchemlett.9b00141
ACS Med. Chem. Lett. XXXX, XXX, XXX−XXX